ELSEVIER

Biophysical Chemistry 64 (1997) 271–287

Biophysical Chemistry

Effects of NaCl on the linkages between O_2 binding and subunit assembly in human hemoglobin: titration of the quaternary enhancement effect

Michael L. Doyle [a], Jo M. Holt [b], Gary K. Ackers [b,*]

[a] *Macromolecular Sciences Department, SmithKline Beecham Pharmaceuticals, King of Prussia, PA 19406, USA*

[b] *Department of Biochemistry and Molecular Biophysics, Washington University School of Medicine, St. Louis, MO 63110, USA*

Received 16 July 1996; accepted 11 September 1996

Abstract

Oxygen binding by human hemoglobin (Hb) and the coupled reactions of dimer–tetramer assembly were studied over a range of NaCl concentrations (from 0.08 M to 1.4 M) at pH 7.4 and 21.5°C. A strategy of multi-dimensional analysis was employed [G.K. Ackers and H.R. Halvorson, Proc. Natl. Acad. Sci. U.S.A., 91 (1974) 4312] to optimize the resolution of the contributions to cooperativity and their heterotropic salt linkages at each stoichiometric degree of O_2 binding. A wide range of Hb concentration was utilized at each [NaCl] in which O_2-linked subunit assembly reactions contributed significantly to the positions and shapes of the binding isotherms. Kinetic determinations yielded forward and reverse rate constants for assembly of the unligated species. Amplitudes for the assembly rate data had concentration dependences in agreement with the independently determined dimer–tetramer assembly constants of oxyhemoglobin. Concentration-dependent binding isotherms were analyzed, in combination with the kinetically determined equilibrium constants, to yield salt-linked components of cooperativity at the four stages of oxygenation.

The principal results of this study were as follows. (i) Assembly of fully oxygenated Hb tetramers is opposed by NaCl; the dimer-to-tetramer equilibrium constant becomes two orders of magnitude less favorable over the [NaCl] range 0.08 M to 1.4 M. By contrast, for deoxy-Hb the assembly equilibrium constant is reduced only two-fold. (ii) Oxygen binding to dimers is non-cooperative over the entire salt range, whereas dimer affinity is slightly favored by increasing the NaCl concentration. (iii) Overall affinity of tetramers for O_2 is opposed by NaCl, becoming an order of magnitude less favorable over the range employed. Most of this decrease occurs at the fourth binding step, which shows a large, salt-mediated quaternary enhancement effect; i.e., the assembly of dimers into tetramers at 0.08 M NaCl is accompanied by an eight-fold increase in O_2 affinity. (iv) The quaternary enhancement effect at the last O_2-binding step is titrated progressively by salt until it reaches a negligible value near the highest [NaCl] of this study. The lowest [NaCl] condition (0.08 M) elicits the greatest tetramer cooperativity with the largest maximal Hill coefficient and the greatest suppression of intermediates. Possible origins and mechanistic implications of these phenomena are considered.

Keywords: Cooperative binding; Hemoglobin; Quaternary enhancement; Regulation; Subunit assembly

Abbreviations: DPG, diphosphoglycerate; HbA_0 (or Hb), human hemoglobin major component; NaCl, sodium chloride; Na_2EDTA, disodium ethylenediaminetetraacetic acid; Tris, tris(hydroxymethyl)aminomethane

* Corresponding author.

PII S0301-4622(96)02235-1

1. Introduction

Physiological chloride has long been recognized as a heterotropic allosteric effector of hemoglobin (Hb), with an overall role of reducing the affinity for O_2 (cf. [1–5]). In addition, salt concentration is a generally useful probe of multi-subunit systems because it can modulate protein–protein interactions through specific ion binding events [6], general charge effects, or, at high concentration, by altering the chemical potential of water [7–9]. Additional interest in the connections between oxygenation, salt binding and dimer–dimer interactions comes from recent findings: (a) fully ligated human Hb can be crystallized under low salt conditions with a "third quaternary structure", designated R2 or Y [10,11], whereas at high salt levels it is found in the classical R quaternary structure [12]; (b) chloride neutralization of positive charge clusters within the tetramer's central cavity has been implicated in modulation of O_2 affinity [13–15]; and (c) detailed features of the Hb mechanism discovered using O_2 analogs and metal-substituted hemes are of importance to compare with the corresponding properties of the native FeO_2 system (cf. [16–20]).

The measurement of oxygen-linked dimer–tetramer assembly affords a sensitive probe of allosteric properties [21–25]. Cooperative oxygen binding by Hb both promotes a global rearrangement of the interface between αβ dimers within the tetramer (i.e., the T → R quaternary switch; cf. [12,26]), and also generates quaternary-linked tertiary conformational strain that is released by the T → R switch [16,27–29]. In this study, the dependences of dimer–tetramer assembly reactions on [NaCl] have been determined for Hb molecules at each stoichiometric degree of oxygenation ($i = 0$, 1, 2, 3, 4). Simultaneously, the four tetrameric O_2-binding constants and the two dimeric binding constants have also been resolved as a function of [NaCl]. The general strategy employed here [21,22] was used previously to characterize the subunit interactions that regulate oxygen-binding affinity and cooperativity over a range of thermodynamic variables, including protein concentration [30], temperature [31,32], and pH [23,33]. This strategy has also been used to elucidate the O_2-binding-linked subunit assembly reactions of Hb containing cobalt-substituted hemes [34] and, at varying levels of detail, with over 65 mutant or chemically modified species [29,35–38].

1.1. Subunit assembly and oxygenation

The linkage reactions of stoichiometric oxygenation at the heme sites and the assembly of dimers into tetramers are depicted in Scheme (1)

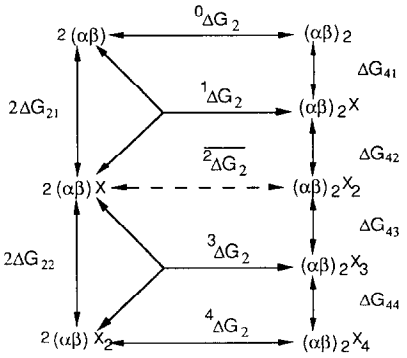

(1)

Standard free energies ΔG_{ni} pertain to reaction equilibria represented by the adjacent arrows (see Appendix A for exact definitions; see ref. [20] for the corresponding system of 10 "ligation microstates"). The dashed arrow at the doubly ligated tetramer indicates an average over the four configurational isomers which contribute to the net assembly free energy, $\overline{{}^2\Delta G_2}$ [21]. The values ${}^1\Delta G_2$ and ${}^3\Delta G_2$ each reflect an average over two "microstate reactions" (i.e. for initial binding to the α or β hemesites), and ${}^0\Delta G_2$ and ${}^4\Delta G_2$ each pertain to a single reaction. Research using O_2 analogs (CO, CN) and metal-substituted hemes that mimic FeO_2 [19,20,39–41] has reinforced the fundamental discovery [24] that specific configurational isomers of the doubly ligated species can have very different cooperativity properties (cf. [16,25,42]). Nevertheless, elucidation of the linkages between O_2 binding and subunit assembly at the stoichiometric level provides important constraints and insights into mechanistic issues that must be compared with the more detailed behavior resolved by the oxygenation analogs.

Resolution of the dependences of parameters in Scheme 1 on an appropriate set of linked variables permits the multiple equilibrium processes that comprise the Hb allosteric mechanism to be deconvoluted at each of the four O_2-binding stages. This

strategy is based on the following rationale [21,22,36]. (1) Oxygenation-induced interactions that generate cooperativity within the Hb molecule are decoupled by dissociation of the tetramers into dimers. (2) The difference δ_{4i} between assembly free energy of a tetramer with i bound oxygens and that of the unligated molecule measures the contribution of subunit interactions which accompany binding of the i oxygens onto the tetramer's α and β subunits. In principle these cooperativity effects could be determined either as differences in successive binding constants or, reciprocally, as differences in successive dimer–tetramer assembly constants (corrected in each case for the appropriate statistical factors). The "cooperative free energies" δ_{4i} (also termed "regulatory energies," cf. [36]), which may be determined by subunit assembly measurements, will include contributions from the tertiary and quaternary structural transitions that accompany ligation, and from any changes in solvent interactions or in O_2-linked binding of heterotropic ligands (Bohr protons, CO_2, DPG, and chloride). The net free energy ΔG_{4i} for binding i oxygens to the tetramer may thus be represented as:

$$\Delta G_{4i} = \langle \Delta G \rangle_{4i} + \delta_{4i} \tag{2}$$

where $\langle \Delta G \rangle_{4i}$ is a free energy arising from the intrinsic site binding constants k_α and k_β, averaged over all configurations of occupied heme sites when i oxygens are bound (defined below for the various cases by Eqs. (5a), (5b), (5c), (5d), (5e), (5f), (5g) and (5h)). The binding constants of dissociated dimers have frequently provided a practical means of evaluating $\langle \Delta G \rangle_{4i}$ [21,22].

1.2. Relationships to the binding isotherms and other cooperativity parameters

The relationships between Eq. (2) and parameters of the linkage Scheme 1 can be specified by considering the nested thermodynamic cycles, which each include ${}^0\Delta G_2$ and one of the successive ${}^i\Delta G_2$ terms ($i = 1, 2, 3, 4$) with the appropriate combinations of binding free energies on the left hand and right hand sides of each cycle.

Transformation of the free energy terms in Scheme 1 into standard equilibrium constants [i.e., $K = \exp(-\Delta G/RT)$] yields

$$K_{4i} = \bar{K}_{4i} \exp(-\delta_{4i}/RT) \tag{3}$$

where K_{4i} is the standard Adair binding constant for reacting i oxygens with heme sites on the Hb tetramer (cf. [43,44]) and $\bar{K}_{4i}$ is the pertinent combination [36] of k_α and k_β values (given explicitly in Eqs. (5a), (5b), (5c), (5d), (5e), (5f), (5g) and (5h) below). By path independence of free energy, the ratio $K_{4i}/\bar{K}_{4i}$ for each of the nested cycles will equal ${}^iK_2/{}^0K_2$, so that

$${}^iK_2/{}^0K_2 = \exp(-\delta_{4i}/RT) \tag{4}$$

Then, defining ${}^iK_c \equiv {}^iK_2/{}^0K_2$, the Adair constants K_{4i} (i.e., uncorrected for statistical factors) are transformed into Eqs. (5a), (5c) and (5e) and Eq. (5g) for the general case, or alternatively into Eqs. (5b), (5d) and (5f) and Eq. (5h) when the dimeric sites have identical intrinsic binding affinities: $k_\alpha = k_\beta \equiv k_d$.

$$K_{41} = (2k_\alpha + 2k_\beta)({}^1K_c) \tag{5a}$$

$$K_{41} = 4k_d({}^1K_c) \tag{5b}$$

$$K_{42} = (4k_\alpha k_\beta + k_\alpha^2 + k_\beta^2)({}^2K_c) \tag{5c}$$

$$K_{42} = 6(k_d)^2({}^2K_c) \tag{5d}$$

$$K_{43} = (2 \cdot k_\alpha^2 \cdot k_\beta + 2k_\alpha \cdot k_\beta^2)({}^3K_c) \tag{5e}$$

$$K_{43} = 4(k_d)^3({}^3K_c) \tag{5f}$$

$$K_{44} = (k_\alpha^2 k_\beta^2)({}^4K_c) \tag{5g}$$

$$K_{44} = (k_d)^4({}^4K_c) \tag{5h}$$

These relationships show explicitly how the free energy costs of tetrameric cooperativity which are "paid" at the stoichiometric binding reactions may be evaluated through experimental determinations of ${}^iK_2$ and ${}^0K_2$. The stoichiometric cooperativity parameters may thus be found by determining the assembly free energies of linkage Scheme 1, as Eq. (4) may be written

$$\delta_{4i} = -RT \ln({}^iK_c) \tag{6}$$

An important issue is the relationship of these cooperativity parameters to the standard tetrameric binding isotherm $\bar{Y}_4$:

$$\bar{Y}_4 = \frac{K_{41}x + 2K_{42}x^2 + 3K_{43}x^3 + 4K_{44}x^4}{4(1 + K_{41}x + K_{42}x^2 + K_{43}x^3 + K_{44}x^4)} \tag{7}$$

where x is the O_2 concentration (cf. [43,44]). By use of Eqs. (5a), (5b), (5c), (5d), (5e), (5f), (5g) and (5h), this isotherm may be formulated explicitly in terms of the free energy costs of cooperativity. When α and β subunits have the same intrinsic affinity k_d (as found with the dissociated dimers over a wide range of conditions) the tetramer binding isotherm can be written

$$\bar{Y}_4 = \frac{({}^1K_c)(k_d x) + 3({}^2K_c)(k_d x)^2 + 3({}^3K_c)(k_d x)^3 + ({}^4K_c)(k_d x)^4}{1 + 4({}^1K_c)(k_d x) + 6({}^2K_c)(k_d x)^2 + 4({}^3K_c)(k_d x)^3 + ({}^4K_c)(k_d x)^4} \tag{8}$$

Extension of these functions to account for the composite binding isotherm of the linked dimer–tetramer system (Eq. (A1)) is accomplished by noting that the dimeric polynomials of Appendix Eq. (A1) will be: $Z_2 = 1 + k_d x + (k_d x)^2$, and $Z_2' = k_d x + 2(k_d x)^2$. Likewise, the Hill coefficient n_H for the tetrameric species (Eq. (A7) or Eq. (A8)) may be readily calculated as a function of the stoichiometric cooperativity parameters ${}^iK_c$ along with the intrinsic affinity k_d by substituting Eq. (8) into Eq. (A8). The Hill coefficient, traditionally taken from an O_2-binding isotherm at half-saturation $\bar{Y} = 0.5$, or at its maximal value $n_{H,max}$ provides only minimal information on the system's cooperativity compared with a resolved set of the four Adair constants K_{4i} [43,44]. These constants in turn provide much less information than the nine site-specific constants for binding or assembly (cf. [20]).

Each δ_{4i} reflects the gain or loss in "strength of interaction" between the $\alpha^1\beta^1$ and $\alpha^2\beta^2$ dimeric units that are globally reoriented in the O_2-driven $T \rightarrow R$ quaternary switch [12,26,74,75]. A determined set of δ_{4i} values ($i = 1, 2, 3, 4$) thus reveals how much the free energy of dimer–dimer association is altered (and in what direction) at each of the four oxygen-binding steps. This perspective on the molecular interactions that contribute to cooperativity bears a complementary relationship to the (equivalent) view in which ratios of the (normalized) Adair binding constants ($K_{4i}/\bar{K}_{4i}$) have traditionally been used to define the cooperativity sequence. As shown by Eqs. (3) and (4), the two approaches are entirely equivalent, but they emphasize different facets of the same phenomenon. It is thus important to recognize that cooperative free energies δ_{4i} determined from oxygenation-induced changes in subunit association need not reflect solely the structural alterations at the subunit interfaces; in principle they may also reflect structural alterations at ligated heme sites distant from the interfaces, or alterations propagated through the tertiary structures of the oxygenated subunits.

2. Materials and methods

2.1. Materials

Human HbA_0 was purified from hemolysates of freshly drawn blood (MLD) by the method of Williams and Tsay [45], which removes organic phosphates and minor Hb components by DEAE anion exchange. The final HbA_0 preparation contained 1.0% oxidized hemes, based on spectral changes upon addition of KCN. All measurements were performed in 0.1 M Tris base, 1 mM Na_2EDTA at 21.5°C, pH 7.40, and specified [NaCl]. Here [NaCl] refers to the concentration of chloride needed to titrate the Tris base buffer to pH 7.4 (0.08 M) plus an amount added as [NaCl]. Human haptoglobin type 2-2 was purified as described [46,47].

2.2. Deoxy dimer–tetramer association rates

The equilibrium constant ${}^0K_2$ for dimer–tetramer assembly of deoxy Hb was determined from measurements of the forward and reverse reaction rates. Association kinetics of the dimers were measured by the rapid-mixing procedure of Kellett and Gutfreund [48]. As the dilute oxygenated solutions of Hb contained mixtures of tetramers and dimers, mixing them with deoxygenated buffer containing 0.2–0.4% sodium dithionite scavenges the O_2, leading to a rapid deoxygenation of Hb ($t_{1/2} \approx 30$ ms). This is immediately followed by net assembly of dimers into tetramers, since the association equilibrium constant for deoxy tetramers is much larger than that of oxygenated species. This deoxy assembly reaction is

monitored in the Soret band at 430 nm. Dimer–tetramer association kinetics obey the following integrated second-order rate law (cf. [47,49])

$$A_t = A_\infty - \frac{\Delta A}{D_0 k_f t + 1} \quad (9)$$

where A_t and A_∞ are the absorbances at respective times t and infinity, ΔA is the observed amplitude of reaction $(A_\infty - A_0)$, and k_f is the forward rate constant for dimer–tetramer assembly [1]. At the start of second-order assembly, the dimer concentration D_0 is governed by the equilibrium constant, $^4K_2$, for assembly of fully oxygenated tetramers and by the total Hb concentration, P_t

$$D_0 = \frac{-1 + \sqrt{1 + 4P_t {}^4K_2}}{4(^4K_2)} \quad (10)$$

By Eqs. (9) and (10), the ratio $\Delta A/A_\infty$ is directly proportional to the fraction f_2 of Hb in dimeric form at the initial condition of each experiment [2]. The relationships in Eq. (9) and Eq. (10) provide a means of testing the kinetic reaction model for subunit assembly, as $^4K_2$ was measured independently by median analysis of the binding isotherms [22,50]. Our kinetically derived results were nearly identical with $^4K_2$ values from high-precision osmotic pressure measurements (Table 3) over the same [NaCl] range [51], and also with results from analytical gel chromatography [33].

2.3. Tetramer–dimer dissociation kinetics of deoxy-Hb

Dissociation rate constants were measured by the haptoglobin technique [37,46,47]. Solutions of Hb and haptoglobin were deoxygenated for 1 h inside an anaerobic chamber (Coy Laboratories). Dithionite (sodium hydrosulfite, or Vertex D, from Hoechst Celanese) was added to the Hb solution to 0.01% w/v immediately prior to filling each side of a split cell mixing cuvet. The glass-stoppered cuvet was sealed inside the anaerobic chamber with deoxygenated stopcock grease. Reaction was initiated by manual mixing, and N_2 (g) was continually flushed over the glass stoppers to prevent diffusion of oxygen into the cuvet. Time courses monitored at 430 nm by a Cary 219 spectrophotometer followed the first-order rate equation

$$A_t = A_\infty + (A_0 - A_\infty)\exp(-k_r t) \quad (11)$$

where absorbances A_0 and A_∞ pertain to initial and infinite times, respectively, and k_r is the rate constant for tetramer–dimer dissociation. The ratio of k_f (Eq. (9)) to k_r provides a determination of the equilibrium constant $^0K_2$ for dimer–tetramer assembly of the unligated species.

2.4. Oxygen binding

Oxygen-binding isotherms were measured with a continuous-flow spectrophotometric method ([30,52]; see [23] for protocols of the present study). The Hb sample was equilibrated in the cell against humidified O_2 at one atmosphere pressure. Deoxygenation was effected by flushing the stirred sample with humidified N_2 gas (Linde O_2-free grade). Fractional saturation by O_2 was monitored with a Cary 4 spectrophotometer at $\lambda = 415$ nm for 5.77 μM heme (or lower), at $\lambda = 600$ nm for 80 μM (or above) and at 415 nm for the remaining data. Temperature in the sample cell was regulated within ±0.02°C by a Tronac PTC-36 temperature controller (Tronac, Inc., Orem, UT), and was determined by a thermistor probe-linked digital thermometer (Cole-Parmer 8502-20). O_2 activity was measured with a Beckman 39065 O_2 electrode probe with a Nicolet model 3091 digital oscilloscope. Absorbances versus O_2 activity were sampled in equal logarithmic increments of the latter. These measurements were in the range below 2.0 AU. Accuracy of the Cary 4 spectrophotometer was determined to be at least 0.15% relative error at 4.17 AU based on gravimetric dilutions of dissolved potassium chromate [53].

[1] This reaction follows the second-order expression

$$k_f t = \frac{1}{D} - \frac{1}{D_0}$$

where D_0 and D are dimer concentrations at the initial time ($t = 0$) and at time t, respectively. The fraction f_2 of Hb in dimeric form at the initial condition of each experiment is $D_0[\Delta A / A_\infty]$, so that $D_0 k_f t = (A_\infty / \Delta A) - 1$, which is equivalent to Eq. (9).

[2] This proportionality constant accounts for the difference in extinction between dimers and tetramers divided by the extinction coefficient of tetramers, $(\epsilon^T - \epsilon^D)/\epsilon^T$ (approximately 0.10 at 430 nm).

Multiple-wavelength O_2 equilibrium curves were measured at 0.70 M [NaCl] with the Cary 4 instrument by scanning 50 nm wavelength segments (either from 390 to 440 nm or from 550 to 600 nm) at 15 nm s^{-1} while collecting absorbance data in intervals of 1 nm. This scan rate was verified not to skew the sharpest of the Hb absorbance peaks (oxygenated, 415 nm) to within spectrophotometric noise at 1 AU. Each scan was completed within 3.4 s, so the mean O_2 activity reading of the electrode (over the 50 values measured during each scan) could be taken as the pertinent value for each wavelength in a given scan. Scans were performed once per minute until the sample was essentially deoxygenated. The data matrix for each O_2 equilibrium curve, consisting of approximately 40 O_2 activities × 50 wavelengths, was then analyzed by singular value decomposition (see [54–57]). Results of these analyses indicated only a single transition, so that no spectral intermediates were taken into account during subsequent analyses. The first columns of each of the "V" matrices were globally analyzed for subunit assembly and O_2-binding free energies, as in the single-wavelength absorbance data at the other salt conditions of this study. The observation of only a single optical transition under the conditions of this study is not inconsistent with previous findings of multiple transitions at lower wavelength with samples containing IHP [56].

While oxidation of hemoglobin samples was minimized by use of an enzymic reductase system [58], the typical accumulation of oxidized Hb during the entire deoxygenation–reoxygenation process was 1–2% (corresponding to the expected levels of irreversible denaturation over the prolonged stirring of dilute Hb samples in this experiment). Reversibility was evaluated by comparing deoxygenation and reoxygenation absorbance traces: these showed return to the initial absorbance to within 1–2% of the total absorbance change.

2.5. Analysis strategy

Global regression analysis of the oxygenation isotherms determined over a range of Hb concentration was governed by Eq. (12)

$$A(X_i) = A_0 + (A_\infty - A_0)\bar{Y}(X_i) \qquad (12)$$

where $A(X_i)$ is the ith observed absorbance value at O_2 activity X_i, $\bar{Y}(X_i)$ is fractional saturation at X_i (Appendix Eq. (A1)); A_0 and A_∞ are the asymptotic absorbance values for zero and infinite O_2 activities, respectively.

The functional form of the fitting equation for $\bar{Y}$ (Eq. (A1)) contains the Gibbs free energies corresponding to equilibrium constants K_{41}, K_{42}, K_{43}, ${}^4K_2$, and k_{22}. Although independent sets of thermodynamic linkages sufficient to define Scheme 1 may be chosen according to multiple combinations of parameters [22], the combination used in the present study was chosen for convenience of the data measurement sequence to allow independent analysis of the O_2-binding equilibrium and also the deoxygenated dimer–tetramer assembly free energy, ${}^0\Delta G_2$. Thus, equilibria involving the deoxy dimer (${}^0K_2$ and k_{21}) were fully determined from conservation of energy imposed by resolved values of the above fitting parameters and the independently measured value of ${}^0K_2$. It is of particular interest that the first and second O_2-binding steps of the αβ dimer were determined by essentially independent measurements. This approach affords the most explicit tests to date of cooperativity for the dissociated dimers.

Following regression analysis, the data were also converted to $\bar{Y}$ values for illustrative purposes. Least-squares analyses utilized the program NONLIN [59], which employs a modified Gauss–Newton algorithm to find most probable values of the adjustable parameters, and evaluates the upper and lower confidence limits by searching variance space for an F-statistic corresponding to 67% confidence limits [22,59]. Standard errors were propagated for all parameters not directly fitted (cf. [60]). Data points were weighted equally in terms of absorbance, based on extensive analyses of this specific fitting problem [61,62].

Median ligand activities (Appendix, Eq. (A5)) were determined by first fitting the data for each isotherm to a series of multiple-order binding polynomials. It was found that an empirically determined fourth degree polynomial function provided adequate initial description of each O_2 equilibrium curve for accurate determination of its median value. Extensive simulation and analyses indicated no loss of accuracy using these functions for median positions, whereas the Adair constants, which are sensitive to

curve shape, necesssitated use of the refined isotherms.

2.6. O_2 solubilities

The solubility of O_2 in water depends strongly on NaCl concentration; conversions from O_2 partial pressures to molarities of dissolved O_2 were made with the following Henry's law constants [63,64]: 1.81×10^{-6} (0.08 M NaCl), 1.66×10^{-6} (0.35 M NaCl), 1.49×10^{-6} (0.70 M NaCl), and 1.21×10^{-6} (1.40 M NaCl).

3. Results

3.1. Parameters for dimer–tetramer assembly of deoxy-Hb

Fig. 1 shows representative second-order plots for the time courses of deoxy dimer–tetramer assembly from stopped flow experiments at the [NaCl] values employed in this study. Inverse fractions of the

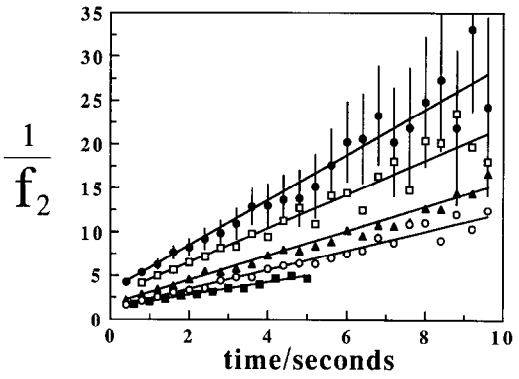

Fig. 1. Second-order plots for kinetics of dimer–tetramer assembly at various NaCl concentrations: 0.08 M (●), 0.18 M (□), 0.35 M (▲), 0.70 M (○) and 1.4 M (■). Heme concentrations were 8.20, 7.90, 5.99, 7.81 and 6.00 μM, respectively. Data plotted vs. time are the inverse fraction of Hb dimers, $1/f_2$, calculated as $1/f_2 = [\Delta A_\infty(\epsilon^T - \epsilon^D)/\epsilon^T]/(A_t - A_\infty)$. Lines represent best-fit second-order rate constants (Table 1) obtained by fitting absorbance data to Eq. (9). Bars show relative error arising from transformation of absorbance data into the second-order plot, and correspond to a constant spectrophotometric noise of 0.0001 AU. Conditions: 0.1 M Tris base, 1 mM Na_2EDTA, 21.5°C and pH 7.40, with additional NaCl to obtain the concentrations given above.

dimeric species $1/f_2$ were calculated by Eqs. (9) and (10) as the absorbance ratio $\Delta A/A_{00}$ multiplied by the spectral range factor (see Materials and methods, Section 2). Table 1 lists the best-fit second-order rate constants k_f for dimer–tetramer assembly obtained by fitting to Eq. (9) at each NaCl concentration.

The protein concentration dependences of amplitudes from the dimer–tetramer assembly kinetics (data points) are shown in Fig. 2 together with the initial fractions ${}^4f_2$ of dimeric Hb (solid curves). These curves were calculated using the equilibrium constants ${}^4K_2$ resolved by median analysis of the oxygen-binding isotherms (Section 3.2, below) while holding ${}^0K_2$ at its independently determined value in each case. Concentration dependences of amplitudes for the assembly rate data are seen to be in conformity with the mass action curves (Fig. 2) that were simulated from the independently determined equilibrium constants ${}^4K_2$. Such agreement between equilibrium parameters and kinetic data argues that both methods are quantitatively reflecting the same reaction process [50].

Fig. 3 shows the tetramer to dimer dissociation reactions as monitored by the haptoglobin kinetics method. First-order plots at each [NaCl] were analyzed by Eq. (11) to yield the k_r values listed in Table 1. These rate constants, and the equilibrium values of ${}^0K_2$ obtained as ratios of k_f values to their corresponding k_r values, provided the equilibrium constants and free energies ${}^0\Delta G_2$ of dimer–tetramer assembly (rightmost column). These results show that the stability of the unligated tetramer is altered by only 500 cal mol^{-1} over the [NaCl] range of this study, in confirmation of earlier determinations [33].

3.2. Overall energetics of subunit assembly and O_2 binding for dimers and tetramers

The median partial pressure X_{med} for each isotherm at a particular Hb concentration measures the thermodynamic work of oxygenating all heme sites in solution (dimers and/or tetramers). An exact relationship defining the heme concentration dependence of median partial pressures for the composite system (Eq. (A5); [22]) was employed to obtain values of ${}^4K_2$ and K_{44} (the equilibrium constant for

Table 1
[NaCl] dependence of forward and reverse rates for dimer–tetramer assembly of deoxygenated Hb [a]

[NaCl]/M	$k_f/(M^{-1}\,s^{-1})$ [b]	$k_r(s^{-1})$ [c]	$-RT\ln(k_f/k_r)$kcal
0.08	1.2×10^{6}	2.1×10^{-5}	-14.51 ± 0.2
0.18	6.0×10^{5}	1.1×10^{-5}	-14.47 ± 0.2
0.35	5.0×10^{5}	7.8×10^{-6}	-14.57 ± 0.2
0.70	3.0×10^{5}	7.5×10^{-6}	-14.29 ± 0.2
1.40	2.3×10^{5}	8.8×10^{-6}	-14.04 ± 0.2

[a] 0.1 M Tris base, pH 7.40, 21.5°C, 1 mM Na_2EDTA.
[b] Standard errors on k_f are approx. 30%.
[c] Standard errors on k_r are approx. 10%.

overall tetramer O_2 binding) while holding ${}^0K_2$ at the kinetically determined values described above. A rigorous analysis of this type is especially valuable for highly cooperative, subunit-dissociating systems such as human Hb, because it permits the overall parameters to be determined accurately prior to the more challenging task of evaluating detailed shapes of the binding curves by nonlinear global analysis.

Fig. 4 shows the median partial pressures of O_2 for each salt condition, measured over a range of Hb concentration. By means of Eq. (A5), the parameter K_{44} is well determined at any single Hb concentration, and the parameters ${}^4K_2$ and ${}^0K_2$ are reflected in the curvature shown. The lower concentration limit for these studies was approximately 500 nM heme, and ${}^0K_2$ was determined independently as described above. Its value was subsequently held fixed in using Eq. (A6) and Eq. (A5) for regression analysis [15] via Eq. (A5). The resulting parameter estimates for K_{44} and ${}^4K_2$ from fitting the median data in Fig. 4 were then justifiably used as initial estimates for the more detailed global shape analysis described below. The free energies $\Delta G_4 = -RT\ln K_{44}$ and ${}^4\Delta G_2 = -RT\ln({}^4K_2)$ are given in Table 2 along with free energies ΔG_2 of saturating the dimers. The ΔG_2 values were obtained by utilizing the path independence of free energies and the determined values of ${}^0\Delta G_2$, ${}^4\Delta G_2$ and ΔG_4. It can be seen (Table 2) that the effect of [NaCl] on dimer affinity is very small,

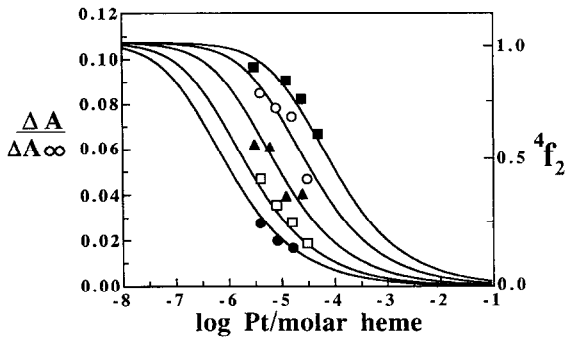

Fig. 2. Correspondence between amplitudes from dimer to tetramer assembly kinetics and the initial fractions of dimeric Hb. [NaCl] values were: 0.08 M (●), 0.18 M (□), 0.35 M (▲), 0.70 M (○) and 1.4 M (■). Solid curves are calculated from dimer–tetramer equilibrium constants ${}^4K_2$ resolved by median analyses according to Eq. (A5)–A7 and the kinetically determined values of ${}^0K_2$. The left ordinate is the ratio of the amplitude, ΔA, for the kinetics of dimer–tetramer assembly to the total absorbance difference, ΔA_∞ (Eq. (9)). Left ordinate intersects limiting values at low [Hb] giving the fractional change in absorbance at 430 nm between pure deoxygenated dimers and tetramers. The right ordinate is the fraction of dimers, ${}^4f_2$, present in the initial (fully oxygenated) state.

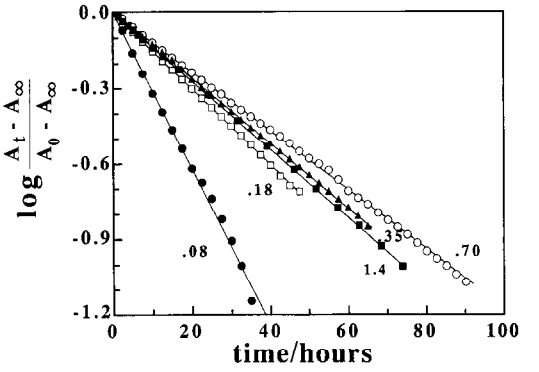

Fig. 3. First-order plots of Hb tetramer–dimer dissociation kinetics at [NaCl] values: 0.08 M (●), 0.18 M (□), 0.35 M (▲), 0.70 M (○) and 1.4 M (■). Lines represent best-fit parameters from Eq. (12). Conditions as in Fig. 1. Protein concentrations were 2–4 μM heme. Human haptoglobin type 2-2 was used in 2-fold excess.

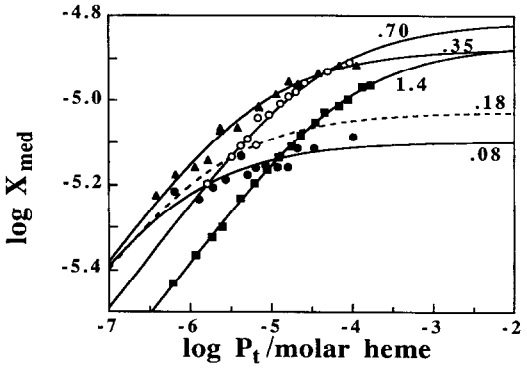

Fig. 4. Dependence of median O_2 partial pressure, X_m (Torr units), for oxygenation as a function of Hb concentration, P_t, at [NaCl] values: 0.08 M (●), 0.35 M (▲), 0.70 M (○) and 1.4 M (■). Solid curves show best fit regression analyses to Eq. (A5).

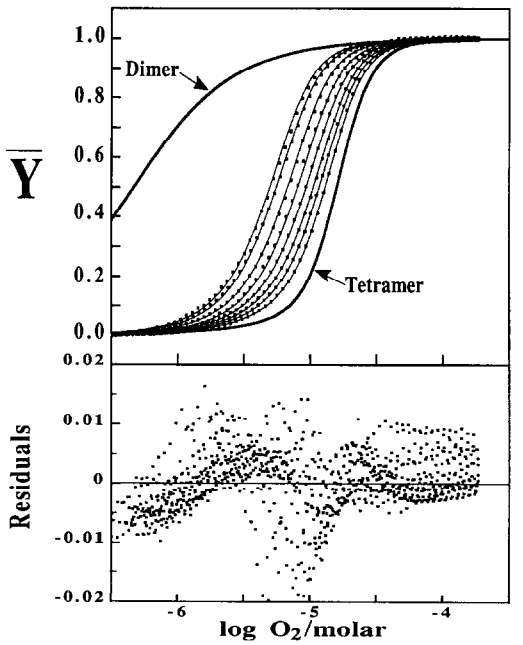

Fig. 5. Binding isotherms (top) at Hb concentrations (right to left): 166 μM, 68.1 μM, 34.7 μM, 17.5 μM, 8.80 μM, 4.12 μM, 1.85 μM and 1.17 μM heme. Conditions: 1.40 M NaCl, 0.1 M Tris base, 1 mM Na_2EDTA, 21.5°C and pH 7.40. Every fifth data point is plotted. Thick curves depict isotherms calculated for pure dimers and tetramers. Other curves represent best fits to Eq. (12) for each total concentration of Hb. Bottom: Residuals in $\bar{Y}$ units for the global fit of 16 isotherms to Eq. (12). Every fifth residual is plotted. Square root of the variance for the global fit was 0.00586 in $\bar{Y}$ units with 4717 degrees of freedom.

with a slightly higher affinity at the highest salt level. Also tabulated are the total cooperative free energies $^4\Delta G_c$ over all four stages of O_2 binding. This quantity, which measures the total free energy cost for binding O_2 to tetramers (relative to that of the non-cooperative dimers), is significantly increased by higher [NaCl].

3.3. Energetics of O_2 binding and subunit assembly for partially oxygenated species

Equilibria involving the intermediate oxygenation stoichiometries (Scheme 1) were determined for each [NaCl] by simultaneous fitting of the binding curves measured over a range of Hb concentration (Eq. (12) and A1). Fig. 5 shows a representative set of oxygenation isotherms for 0.70 M chloride. Best-fit parameters from analyses of similar data series, each taken over a range of [NaCl], are summarized in Table 3. Uncertainties are reported as standard errors, including cases where the confidence intervals were highly asymmetric, such as with ΔG_{42} (especially at high salt) and ΔG_{43} (especially at low salt):

Table 2
Overall O_2-binding and assembly properties of Hb at various salt concentrations determined by median analysis [a]

[NaCl]/M	$^0\Delta G_2$ [b]	$^4\Delta G_2$ [c]	ΔG_4 [c]	ΔG_2 [d]	$^4\Delta G_c$
0.08	−14.51	−8.52 ± 0.3	−27.48 ± 0.10	−16.74	5.99 ± 0.4
0.18	−14.35	−8.05 ± 0.1	−27.10 ± 0.10	−16.69	6.30 ± 0.2
0.35	−14.57	−7.30 ± 0.1	−26.29 ± 0.10	−16.78	7.27 ± 0.2
0.70	−14.29	−6.35 ± 0.2	−25.95 ± 0.15	−16.95	7.94 ± 0.3
1.40	−14.04	−5.88 ± 0.1	−26.03 ± 0.10	−17.20	8.16 ± 0.2

[a] 0.1 M Tris base, pH 7.40, 21.5°C, 1 mM Na_2EDTA. All free energies in kcal.
[b] From the determined rate constants of the forward and reverse reactions.
[c] Determined from regression analysis on Eq. (A5).
[d] $\Delta G_2 = 1/2(^0\Delta G_2 + \Delta G_4 - {}^4\Delta G_2)$

Table 3
Salt dependence of intrinsic O_2-binding and subunit assembly free energies [a]

(A) Dimer–tetramer assembly free energies, $\Delta G'_2$, for tetramers with i oxygens bound/kcal

[NaCl]	$^0\Delta G_2$	$^1\Delta G'_2$	$^2\Delta G'_2$	$^3\Delta G'_2$	$^4\Delta G_2$	$^4\Delta G_2$ [e]
0.08	−14.51 ± 0.2	−11.60 ± 0.3	−8.38 ± 0.5	−7.35 ± 0.6 [d]	−8.55 ± 0.1	−8.7 ± 0.1
0.18 [b]	−14.35 ± 0.1	−11.48 ± 0.2	−8.68 ± 1.3	−7.21 ± 0.4	−8.05 ± 0.1	−8.0 ± 0.1
0.35	−14.57 ± 0.2	−11.43 ± 0.3	−8.08 ± 0.5	−6.51 ± 0.5	−7.30 ± 0.1	−7.3 ± 0.1
0.70 [c]	−14.29 ± 0.2	−11.05 ± 0.3	−7.38 ± 0.6	−6.08 ± 0.5	−6.40 ± 0.1	−6.8 ± 0.1
1.40	−14.04 ± 0.2	−11.06 ± 0.3	−7.09 ± 1.6	−5.80 ± 0.4	−5.85 ± 0.2	−6.1 ± 0.1

(B) Changes in assembly free energy, $\delta\Delta G'_{ij}$, between tetramers with i and j oxygens bound/kcal

[NaCl]	$\delta\Delta G'_{01}$	$\delta\Delta G'_{13}$	$\delta\Delta G'_{34}$	$\delta\Delta G_{04}$
0.08	−2.91 ± 0.3	−4.25 ± 0.7 [d]	+1.20 ± 0.6 [d]	−5.96 ± 0.2
0.18 [b]	−2.91 ± 0.1	−4.80 ± 0.4	+0.83 ± 0.4	−6.28 ± 0.1
0.35	−3.14 ± 0.2	−4.92 ± 0.6	+0.79 ± 0.5	−7.17 ± 0.2
0.70 [c]	−3.24 ± 0.2	−4.97 ± 0.6	+0.32 ± 0.5	−7.89 ± 0.2
1.40	−2.98 ± 0.3	−5.26 ± 0.6	+0.05 ± 0.4	−8.19 ± 0.2

(C) Free energies, $\Delta G'_{4i}$, for the ith tetramer oxygenation step and total free energy for four oxygens

[NaCl]	$\Delta G'_{41}$/(kcal/O_2)	$\Delta G'_{42}$/(kcal/O_2)	$\Delta G'_{43}$/(kcal/O_2)	$\Delta G'_{44}$/(kcal/O_2)	ΔG_4/(kcal/4O_2)
0.08	−5.29 ± 0.1	−5.30 ± 0.4	−7.20 ± 0.8	−9.72 ± 0.6 [d]	−27.48 ± 0.1
0.18 [b]	−5.43 ± 0.1	−5.54 ± 1.3	−6.96 ± 1.1	−9.16 ± 0.4	−27.10 ± 0.1
0.35	−5.20 ± 0.1	−4.98 ± 0.5	−6.88 ± 0.7	−9.12 ± 0.5	−26.17 ± 0.1
0.70 [c]	−5.16 ± 0.1	−4.79 ± 0.5 [d]	−7.09 ± 0.6 [d]	−8.78 ± 0.4	−25.82 ± 0.2
1.40	−5.44 ± 0.1	−4.72 ± 0.5 [d]	−7.14 ± 0.6 [d]	−8.74 ± 0.3	−26.03 ± 0.2

(D) Combined oxygenation energies for the two intermediate steps/(kcal/2O_2)

[NaCl]	$\Delta G'_{4(2+3)}$
0.08	−12.50 ± 0.6
0.18 [b]	−12.50 ± 0.4
0.35	−11.86 ± 0.5
0.70 [c]	−11.88 ± 0.4
1.40	−11.86 ± 0.3

(E) Free energies, $\Delta G'_{2i}$, for the ith oxygenation step of the dimer, total free energies for binding two oxygens, and free energies of quaternary enhancement at the fourth binding step

[NaCl]	$\Delta G'_{21}$/(kcal/O_2)	$\Delta G'_{22}$/(kcal/O_2)	ΔG_2/(kcal/2O_2)	Quaternary enhancement/kcal/O_2)
.08	−8.20 ± 0.2	−8.52 ± 0.2	−16.72 ± 0.1	1.35 ± 0.6
0.18 [b]	−8.35 ± 0.2	−8.35 ± 0.2	−16.69 ± 0.1	0.81 ± 0.4
0.35	−8.34 ± 0.2	−8.33 ± 0.2	−16.67 ± 0.1	0.73 ± 0.5
0.70 [c]	−8.40 ± 0.2	−8.46 ± 0.2	−16.86 ± 0.1	0.36 ± 0.4
1.40	−8.42 ± 0.2	−8.69 ± 0.2	−17.11 ± 0.1	0.14 ± 0.3

[a] 0.1 M Tris base, pH 7.40, 21.5°C, 1 mM Na_2EDTA. Free energies are corrected for statistical degeneracy (Mills et al. [30]).
[b] Values from Chu et al. [23].
[c] From analysis of multiple wavelength O_2 equilibrium data (see experimental procedures).
[d] Confidence intervals for these cases are highly asymmetric (see Results, Section 3).
[e] Determined by osmotic pressure measurements (Schonert and Stoll [51]).

in these cases the lower negative confidence limit may not be determined, but the upper negative limit is well determined within the standard errors reported. Typically 10–12 isotherms were measured over a range of Hb concentration, and one or two of them were discarded as outliers based on examination of residuals from the global fit.

Close examination of the residuals for individual

isotherms indicated only small deviations (approximately 1% of total heme site concentration). These deviations were easily accounted for by the probable amounts of methemoglobin formed at intermediate extents of oxygenation. In order to explore whether bias error originated from equilibrium curves monitored at particular wavelengths, we also measured equilibrium curves as multiple wavelength isotherms.

Fig. 6 shows the stoichiometric tetramer binding free energies (corrected for statistical factors) versus the logarithm of [NaCl]. It is seen that: (a) the affinity for the first O_2 is very similar at each salt concentration; (b) the affinity increases dramatically upon binding the third, and subsequently the fourth, oxygen; and (c) the fourth O_2 binds with higher affinity than that of dissociated dimers. This "quaternary enhancement" effect (i.e., where assembly of the quaternary tetramer is accompanied by an enhanced binding affinity at the fourth step, cf. [32]) is seen to be dependent on salt concentration. The maximal quaternary enhancement (i.e., 1.2 kcal) occurs at 0.08 M NaCl and corresponds to an eightfold larger binding affinity for the assembled tetramer compared with the dissociated dimer. The quaternary enhancement effect is seen to be "titrated" by increasing salt, reaching a negligible value at 1.4 M.

The relationships between oxygen-binding stoichiometry and alterations in assembly free energy are displayed directly in Fig. 7. A progressive reduction of the dimer to tetramer energies is seen upon stepwise oxygenation at low saturations for each salt condition. Upon binding the last oxygen, however, the tetramer is stabilized at low [NaCl]. This effect is diminished with increasing salt until it becomes negligible. It follows that the O_2 affinity at the last binding step of the tetramer is correspondingly enhanced relative to that of the dissociated dimer at low NaCl concentration. These reciprocal manifestations of quaternary enhancement depicted in Figs. 6 and 7 have been found for O_2 binding to normal Hb under a variety of conditions (see Section 4, Discussion).

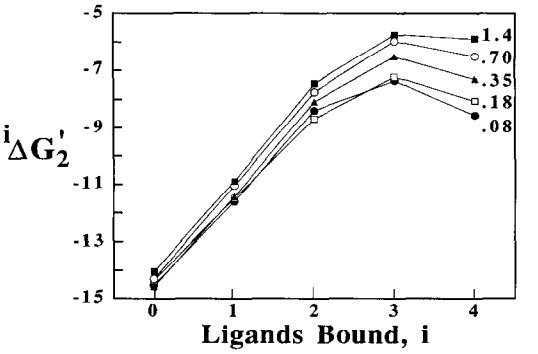

Fig. 7. Dimer–tetramer assembly free energy versus number i of oxygens bound at [NaCl] values: 0.08 M (●), 0.18 M (□), 0.35 M (▲), 0.70 M (○) and 1.4 M (■). Line slopes for the fourth binding step show affinity reversal of dimer assembly (quaternary enhancement) at [NaCl] values of this study.

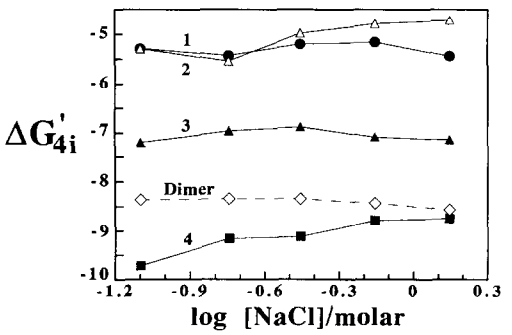

Fig. 6. Intrinsic oxygen-binding free energies versus logarithm of [NaCl] for tetramers: first step (●), second step (Δ), third step (▲), and fourth step (■). For dimers, (◇) is the mean free energy per O_2-binding step.

3.4. Cooperativity within dimers and tetramers

Dimers were found to bind O_2 with no significant cooperativity for all conditions in this study (see values listed in Table 3). These findings are consistent with a wide range of earlier results [30–33,37,38,61,62,75].

Cooperativity within the tetramers at each [NaCl] is portrayed in Fig. 8 as the "Hill slope" (i.e., the Hill coefficient) n_H (Eq. (A9)) plotted against fractional saturation $\bar{Y}_4$. It is seen that the highest values of this function are achieved at the lowest salt concentration, i.e., a maximal n_H of 3.6 was found at 0.08 M NaCl.

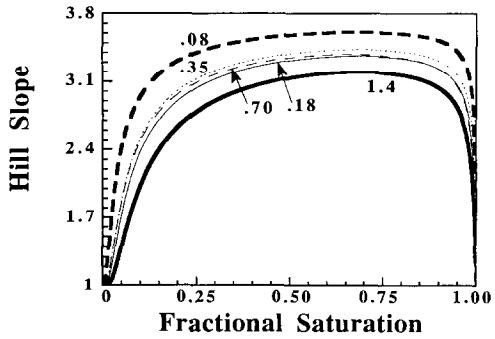

Fig. 8. Maximum slope n_H of the Hill plot versus fractional O_2 saturation of pure tetrameric Hb at NaCl molarities indicated. Maximum Hill slopes are: 0.08 M, 3.61; 0.18 M, 3.38; 0.35 M, 3.43; 0.70 M, 3.40; and 1.4 M, 3.25.

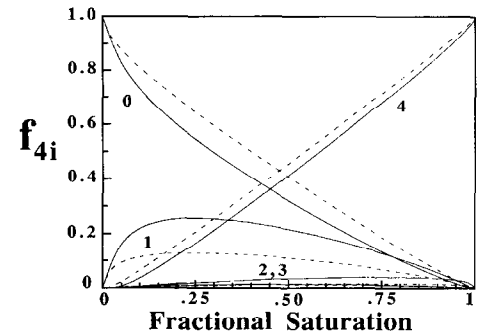

Fig. 9. A: Populations of tetramers with i ligands bound as a function of O_2 saturation. Conditions are as in Fig. 1 with NaCl concentrations of 1.40 M (solid curves) and 0.08 M (dashed curves).

3.5. Effects of [NaCl] on populations of tetrameric species

Fig. 9 depicts the relative abundance f_{4i} of tetrameric species each having i bound oxygens. The dependence of these distributions on salt concentration is illustrated by the differences between solid and dashed lines representing [NaCl] values of 1.4 M (solid lines) and 0.08 M (dashed lines). The effect of salt is to increase the populations of intermediate oxygenation species ($i = 1$, 2, 3) relative to the unligated and fully occupied tetramers. The increased suppression of intermediates arising from lowered [NaCl] is also reflected in the higher values of the Hill slope n_H plotted in Fig. 8.

4. Discussion

A major benefit of explicitly analyzing the linkages between oxygenation and subunit assembly lies in the additional reliability gained from resolving the system's cooperative interactions in multi-dimensional reaction coordinates. The experimental approach is based on four independent techniques in which kinetic and equilibrium measurements of subunit assembly are combined with concentration dependence of oxygen-binding isotherms. A full accounting for the tetramer dissociation at each degree of O_2 binding provides a built-in "correction" for the amplified distortions in apparent tetramer binding constants that can arise in data fitting procedures which may ignore even small populations of dimers in combination with the necessarily small populations of partially ligated tetramers (see [78]). The indeterminate nature of data fitting to cooperative O_2-binding isotherms in the absence of additional dimensions of analysis (e.g., [5,72,79,80]) led Marden et al. [81] to conclude that unique affinities for partially ligated species 'may be impossible'. This conclusion was in accord with our earliest numerical analyses [21,82,22] that led us to develop and exploit the Hb dissociation reactions as an explicit dimension for analysis.

4.1. Cooperative free energies

Whereas Eqs. (A1), (A2), (A3), (A4), (A5), (A6) and (A7) (see Appendix A) have comprised the fitting functions used in this study for analysis of the raw data in relation to parameters of linkage Scheme 1, Eqs. (3), (4), (5a), (5b), (5c), (5d), (5e), (5f), (5g), (5h), (6)–(8) provide an important conceptual "translation" of the linkage parameters into energetic stabilities for tetramers dissociating into dimers as a function of the number i of O_2 molecules bound. The set of cooperative free energies [$\delta_{4i} = -RT \ln({}^{i}K_2/{}^{0}K_2)$ or, equivalently, $\delta_{4i} = RT \ln(K_{4i}/\bar{K}_{4i})$] arguably comprise the most valuable distribution of parameters that can be determined from oxygen-binding analysis: once these have been determined, their various statistical combinations (e.g. the traditional Hill parameter n_H) may be

readily constructed (Fig. 8) for statistical characterization of the population distributions at intermediate degrees of ligation (Fig. 9) as a function of [NaCl].

The assembly free energies resolved in the present study provide a sensitive probe of cooperativity-linked structure changes at the $\alpha^1\beta^2$ interface. That this interface plays a fundamental role in cooperativity has been elucidated by X-ray crystallographic analysis [10–12,26,65,66], and by numerous studies of functional perturbation using mutation and chemical modification (cf. [36,37]). The contributions of inter-subunit interaction to the modulation of net binding affinity and cooperativity are a reflection of the changes in tertiary subunit conformation that are driven by the local heme site binding events. Thus, although the probes used here to drive the Hb system are heme site O_2 binding and subunit association, the observed free energies of O_2 binding also reflect contributions from the tertiary and quaternary structure changes that are driven by the heme site events. Likewise, the measured differences in subunit assembly energetics at the stoichiometric binding steps also reflect the processes of local binding and tertiary conformation change. The driving factors of O_2 chemical potential and of Hb chemical potential have been employed simultaneously in the present study to resolve their heterotropic coupling with respect to NaCl. An extension of the present study to control the chemical potential of water, e.g. by the use of compensating sucrose [8,9,82], should provide additional resolution of the salt vs. water linkages. The present work provides a foundation for such extensions.

4.2. Tertiary constraint and quaternary enhancement

A determined value of δ_{4i} may reflect energetic consequences of O_2-induced conformational strain within the heme pockets and the "allosteric core" of a quaternary T molecule [27]; such strain may be released when the molecule switches to an alternative quaternary structure [28]. Rules for coupling between the configurationally specific Hb ligation states and the acquisition and release of "tertiary constraint" energy have been deduced from studies that resolved these properties for the complete set of ligation species using a variety of O_2 analogs [16,19,20,29].

By contrast, the successive dissociation of O_2 molecules from a fully ligated tetramer (in quaternary structure R or R2) may lead to conformational strain that is also relieved upon switching to an alternative structure. An experimental basis for this concept has been the observation of quaternary enhancement, i.e., an unligated subunit within a tetramer that has an oxy quaternary structure may be energetically disfavored compared with having the same subunit oxygenated. Thus, the O_2 affinity of an assembled protein oligomer may be higher than that of its dissociated subunits.

Such an effect is consistent with the finding of Szabo and Karplus [67] from their model analysis of Roughton's classical oxygenation data [68] that O_2 affinity for the fourth binding step was higher than for isolated subunits. The first experimental observation of quaternary enhancement in a protein system appears to have been made by Nicholas et al. [69]. They found that binding affinity of oxytocin or vasopressin to the dimers of neurophysin was enhanced compared with the corresponding affinities for dissociated neurophysin monomers. A similar effect for the O_2-linked assembly of Hb β subunits into tetramers was discovered independently in two laboratories [70,71]. For normal Hb, the analyses of data bases which reflected both oxygen binding and dimer–tetramer assembly of Hb were found to be compatible with the model-independent binding Eq. (A1) only if the tetramer affinity for the fourth O_2 bound was 3–4-fold higher than that of the dissociated dimers [31]. This effect, which was termed "quaternary enhancement", has been found over a range of temperatures [32] and pH values [23] in addition to the salt ranges of the present study. Apparent quaternary enhancement was also exhibited in the published O_2-binding data of Imai and Yonetani [52] and in the data of Di Cera et al. [72], although neither dimer affinities nor Hb concentration dependences were explicitly determined in those studies.

A very large quaternary enhancement effect has been documented for the mutant human hemoglobin Ypsilanti (β99 asp → tyr) [38], where enhancement is not limited to the last O_2-binding step. A "reverse order" of the binding and assembly free energies in this protein extends over all four steps; fully oxygenated tetramers assemble 170-fold more favorably

than their deoxy counterparts. Reciprocally, the Hb Ypsilanti tetramer has a higher overall O_2 affinity than does its dissociated dimer (which binds with nearly the same affinity as normal dimers). Quaternary enhancement over all four binding steps had also been found in human β_4 tetramers vs. their dissociated monomers [71]. Additional findings of quaternary enhancement have been made with O_2 binding to human Hb substituted with cobaltous hemes in place of ferrous hemes [34], and with CO bound to normal Fe hemes in tetramers containing unligated cobaltous hemes [40].

Arguments against a quaternary enhancement effect in Hb were made by Gibson and Edelstein [73] on the grounds that rate constants from O_2-rebinding experiments were interpreted as not requiring a quaternary enhancement for the equilibrium constant. It was claimed that a particular set of linkage parameters for Scheme 1 might accommodate the concentration-dependent binding isotherms of Mills and Ackers [31,32] without a need for quaternary enhancement. However, when the set of hypothesized parameters [73] was tested for goodness of fit to the actual data the variance of fit was two orders of magnitude poorer than the best (unconstrained) fits to the model-independent linkage scheme which had required the reported quaternary enhancement [31,32]. A subsequent set of the same kinetic parameters [76] also showed, by itself, very little evidence of quaternary enhancement. However, simultaneous analysis of these data in combination with measurements of the other linkage scheme parameters [50] showed that values compatible with both the O_2 equilibrium isotherms and the kinetically derived dimer binding constants required both quaternary enhancement and significant dimer cooperativity. As the absence of significant cooperativity in O_2 equilibrium binding by the dissociated dimers has been supported by numerous studies to date (e.g. [30–33]), it was additionally unclear that the estimated fourth-site O_2-rebinding rates are fully reflective of the equilibrium thermodynamic binding free energy.

It is important to remain concerned over the need for reconciling kinetic parameters with those from equilibrium thermodynamics, and we have taken steps in the present study to address such issues, e.g. by demonstrating that amplitudes of the second-order assembly rate data conform quantitatively to the appropriate mass action law (see Fig. 2), and by employing a data analysis strategy that provides rigorous assessment of possible dimeric cooperativity. It is important to evaluate carefully the robustness and magnitudes of observed phenomena that may be important to the Hb mechanism, even when they are difficult to measure. This is especially underscored by the observation that the entire cooperativity mechanism of the 574 residue Hb molecule is played out within a net free energy of only 6–8 kcal —the equivalent of two or three noncovalent bonds! We believe that earlier concerns regarding the existence of quaternary enhancement should be dispelled by (i) the clearcut demonstration that quaternary enhancement is required to accommodate the multidimensional data bases of high resolution oxygen-binding equilibrium data in combination with O_2-linked subunit assembly measurements over a wide range of conditions; (ii) its discovery at larger scale in the mutant Hb Ypsilanti and in normal Hb β subunits; (iii) the discovery in the present study of an eight-fold affinity enhancement (vs. dimer affinity) for O_2 binding at the fourth tetrameric step of normal Hb; and especially (iv) the concomitant finding that quaternary enhancement may be titrated essentially completely by increasing [NaCl].

The crystallographic observation that low salt conditions may promote fully ligated Hb to adopt the R2 quaternary structure [10,11,77] suggests that changing [NaCl] might shift the population of quaternary structures between R and R2 for fully ligated species in solution [83]. An additional element to this scenario, suggested by the nature of the salt dependence of quaternary enhancement, is that the oxygenated species dominating at low salt (e.g. R2) exhibits quaternary enhancement but the species dominating at high salt (e.g. R) does not. This would be a reasonable hypothesis assuming that crystallization has not introduced structural artifacts. To follow this supposition one step further, is the triply ligated species predominantly in an R quaternary structure, and the fully ligated species in R2? If so, the net energetic change accompanying the transition R → R2 is observed as quaternary enhancement. This is not to imply that the presence of quaternary enhancement *requires* a quaternary structural transition upon ligand binding; cooperativity within the quaternary T tetramer occurs without quaternary transition. How-

ever, it does seem less likely that "tertiary constraint" would be retained in the more relaxed R or R2 structure. Thus, multiple "R-state" structures may exist to generate cooperativity in the fourth ligand binding step, whereas cooperativity within the T structure arises from the generation of tertiary constraint at the initial binding step [16].

It is clear from a large body of work that the tertiary and quaternary switches that control hemoglobin cooperativity may be favored or opposed by non-covalent interactions of the dimer–dimer interface, depending on the ligation state and other conditions. Whereas the energetic contributions of oxygenation-linked tertiary and quaternary conformational changes are not amenable to direct measurement, the present work and related studies on the mutual energetics of oxygenation and subunit assembly offer a useful approach to experimentally defining the constraints under which fundamental elements of the Hb mechanism operate. This approach becomes increasingly valuable as the linkage parameters can be manipulated and explored by varying solvent conditions, allosteric effectors, and with altered hemoglobin structures.

Acknowledgements

This paper is dedicated to the memory of Stanley J. Gill, whose outstanding contributions to the thermodynamics of biological macromolecules were accompanied by warm enthusiasm for the discoveries of other researchers.

The work was supported by NIH Grants R37-GM24486 and PO1-HL51084 and by NSF Grant DMB 9405492.

Appendix A

The fractional O_2 saturation $\bar{Y}$ of an equilibrium solution of Hb is a function of seven independent equilibrium constants [Scheme (1)], the protein concentration P_t (heme units), and the ligand activity [X].

$$\bar{Y} = \frac{Z_2' + Z_4'\left[\sqrt{(Z_2)^2 + 4^0K_2Z_4[P_t]} - Z_2\right]/({}^4Z_4)}{Z_2 + \sqrt{(Z_2)^2 + 4^0K_2Z_4[P_t]}} \quad \text{(A1)}$$

Binding polynomials for dimers (Z_2) and tetramers (Z_4) are

$$Z_2 = 1 + K_{21}[X] + K_{22}[X]^2$$

$$Z_2' = K_{21}[X] + 2K_{22}[X]^2$$

$$Z_4 = 1 + K_{41}[X] + K_{42}[X]^2 + K_{43}[X]^3 + K_{44}[X]^4$$

$$Z_4' = K_{41}[X] + 2K_{42}[X]^2 + 3K_{43}[X]^3 + 4K_{44}[X]^4$$

where prime superscripts indicate first derivatives with respect to the logarithm of [X]. The Adair equilibrium constants, K_{ij}, refer to equilibria between the deoxygenated tetramers ($i = 4$), or dimers ($i = 2$), and the ligation state with a total of j oxygens bound. The stepwise free energies summarized in Table 3 refer to intrinsic, stepwise equilibria, K'_{ij}, for binding the jth O_2 to a dimer or tetramer with $j - 1$ oxygens already bound, and are calculated from the Adair constants and a statistical degeneracy term as

$$k'_{ij} = \left(\frac{j}{i - j + 1}\right)\left(\frac{K_{ij}}{K_{i(j-1)}}\right) \quad \text{(A2)}$$

The free energies for the overall binding of four oxygens to tetramers or two oxygens to dimers are denoted by ΔG_4 and ΔG_2, respectively. Dimer–tetramer assembly equilibrium constants are defined for the jth ligation state of the tetramer as

$${}^jK_2 = \frac{[TX_j]}{[DX_k][DX_l]} \quad \text{(A3)}$$

where $k + l = i$ and k, $l = 0$, 1, 2. Likewise, the corresponding subunit assembly free energies are denoted by ${}^j\Delta G_2$.

The median partial pressure, X_{med}, of an isotherm is a measure of the chemical work for complete

saturation of the macromolecule, and can be found as the partial pressure where the areas above and below the isotherm are equal [44].

$$\int_{[X]=0}^{X_{med}} \bar{Y} d\ln[X] = \int_{[X]=X_{med}}^{[X]=\infty} (1-\bar{Y}) d\ln[X] \qquad (A4)$$

Median analysis of ligand-linked dimerizing systems is especially useful for determining the overall subunit assembly and O_2-binding energies of the system without the need for resolving intermediate oxygenated species from a nonlinear curve-fitting procedure. The median varies with protein concentration P_t according to three overall equilibrium constants: K_{44}, ${}^0K_2$, and ${}^4K_2$ [22,50].

$$X_{med} = \sqrt[4]{\left[K_{44}^{-1} \frac{1-{}^4f_2}{1-{}^0f_2} \exp\left({}^0f_2 - {}^4f_2\right)\right]} \qquad (A5)$$

where

$${}^0f_2 = \frac{\sqrt{1+4[P_t]^0K_2}-1}{2[P_t]^0K_2} \qquad (A6)$$

$${}^4f_2 = \frac{\sqrt{1+4[P_t]^4K_2}-1}{2[P_t]^4K_2} \qquad (A7)$$

The fraction of dimer species for the unliganded and fully liganded systems are designated by ${}^0f_2$ and ${}^4f_2$ respectively.

Statistical averages over properties of the various interacting species are readily calculated from their experimentally resolved values. For example, it is common to discuss the Hill coefficient n_H as an index of cooperativity for the tetrameric binding isotherm $\bar{Y}$, Eq. (7) (see [43])

$$n_H = \frac{d\ln\left[\bar{Y}_4/\left(1-\bar{Y}_4\right)\right]}{d\ln[x]} \qquad (A8)$$

$$n_H = \frac{4\left[\bar{Y}_4^2 - \left(\bar{Y}_4\right)2\right]}{\bar{Y}_4\left(1-\bar{Y}_4\right)} \qquad (A9)$$

The relationship of Eq. (A9) illustrates, upon substituting the right hand side of Eq. (7) for $\bar{Y}_4$, that n_H is a normalized statistical variance of the tetrameric species populations when the mean fraction of occupied sites is $\bar{Y}$ [43]. Because of the equivalent relationship (Eq. (A8)) and its derivative form, n_H has often been referred to as the "Hill slope", which, like $\bar{Y}$, is a continuous function of free ligand activity [X].

References

[1] H.S. Rollema, S.H. de Bruin, L.H.M. Janssen and G.A.J. Van Os, J. Biol. Chem., 250 (1975) 1333.
[2] R.N. Haire and B.E. Hedlund, Proc. Natl. Acad. Sci. U.S.A., 74 (1977) 4135.
[3] K. Imaizumi, K. Imai and I. Tyuma, J. Biochem., 86 (1979) 1829.
[4] G.G.M. Van Beek and S.H. de Bruin, Eur. J. Biochem., 105 (1980) 353.
[5] K. Imai, in Allosteric Effects in Haemoglobin, Cambridge University Press, Cambridge and London, 1982.
[6] S. O'Donnell, R. Mandavo, T.M. Schuster and A. Arnone, J. Biol. Chem., 254 (1979) 12204.
[7] C. Tanford, J. Mol. Biol., 39 (1969) 539.
[8] M.F. Colombo, D.C. Rau and V.A. Parsegian, Science, 256 (1992) 655.
[9] M.F. Colombo and V.A. Parsegian, Proc. Natl. Acad. Sci. USA, 91 (1994) 10517.
[10] F.R. Smith, E.E. Lattman and C.W. Carter, Proteins, 10 (1991) 81.
[11] M.M. Silva, P.H. Rogers and A. Arnone, J. Biol. Chem., 267 (1992) 17248.
[12] J. Baldwin and C.J. Chothia, Mol. Biol., 129 (1979) 175.
[13] H. Ueno and J.M. Manning, J. Protein Chem., 11 (1992) 177.
[14] M.F. Perutz, D.T. Shih and D. Williamson, J. Mol. Biol., 239 (1994) 555.
[15] C. Bonaventura, M. Arumugam, R. Cashon, J. Bonaventura and W.J. Moo-Penn, Mol. Biol., 239 (1994) 561.
[16] G.K. Ackers, M.L. Doyle, D. Myers and M.A. Daugherty, Science, 255 (1992) 54.
[17] M.A. Daugherty, M.A. Shea and G.K. Ackers, Biochemistry, 33 (1994) 10345.
[18] M. Perrella, L. Benazzi, M. Ripamonti and L. Rossi-Bernardi, Biochemistry, 33 (1994) 10358.
[19] Y. Huang and G.K. Ackers, Biochemistry, 35 (1996) 704.
[20] Y. Huang, M. Koestner and G.K. Ackers, accompanying manuscript.
[21] G.K. Ackers and H.R. Halvorson, Proc. Natl. Acad. Sci. U.S.A., 91 (1974) 4312.
[22] M.L. Johnson, H.R. Halvorson and G.K. Ackers, Biochemistry, 15 (1976) 5363.
[23] A.H. Chu, B.W. Turner and G.K. Ackers, Biochemistry, 23 (1984) 604.
[24] F.R. Smith and G.K. Ackers, Proc. Natl. Acad. Sci. U.S.A., 82 (1985) 5347.
[25] J. Holt and G.K. Ackers, FASEB J., (1995) 210.
[26] M.F. Perutz, Nature, 228 (1970) 726.
[27] B.R. Gelin and M. Karplus, Proc. Natl. Acad. Sci. U.S.A., 74 (1977) 801.

[28] B.R. Gelin, A.W. Lee and M. Karplus, J. Mol. Biol., 171 (1983) 489.
[29] V.J. LiCata, P.M. Dalessio and G.K. Ackers, Proteins: Struct., Funct., Genet., 17 (1993) 279.
[30] F.C. Mills, M.L. Johnson and G.K. Ackers, Biochemistry, 15 (1976) 5350.
[31] F.C. Mills and G.K. Ackers, Proc. Natl. Acad. Sci. U.S.A., 76 (1979a) 273.
[32] F.C. Mills and G.K. Ackers, J. Biol. Chem., 254(8) (1979b) 2881.
[33] A.H. Chu and G.K. Ackers, J. Biol. Chem., 256 (1981) 1199.
[34] M.L. Doyle, P.C. Speros, V.J. LiCata, D. Gingrich, B.M. Hoffman and G.K. Ackers, Biochemistry, 30 (1991) 7263.
[35] D. Atha, M.L. Johnson and A.F. Riggs, J. Biol. Chem., 254 (1979) 12390.
[36] D.W. Pettigrew, P.H. Romeo, A. Tsapis, J. Thilet, M.L. Smith, B.W. Turner and G.K. Ackers, Proc. Natl. Acad. Sci. U.S.A., 79 (1982) 1849.
[37] G.W. Turner, F. Galacteros, M.L. Doyle, B. Hedlund, D.W. Pettigrew, B.W. Turner, F.R. Smith, W. Moo-Penn, D.L. Rucknagel and G.K. Ackers, Proteins, 14 (1992) 333.
[38] M.L. Doyle, G. Lew, G.J. Turner, D.L. Rucknagel and G.K. Ackers, Proteins, 14 (1992) 351.
[39] F.R. Smith, D. Gingrich, B.M. Hoffman and G.K. Ackers, Proc. Natl. Acad. Sci. U.S.A., 84 (1987) 7089.
[40] P.C. Speros, V.J. LiCata, T. Yonetani and G.K. Ackers, Biochemistry, 30 (1991) 7254.
[41] Y. Huang, M.L. Doyle and G.K. Ackers, Biophys. J., (1996), in press.
[42] M. Perrella, L. Benazzi, M.A. Shea and G.K. Ackers, Biophys. Chem., 35 (1990) 97.
[43] J.T. Edsall and H. Gutfreund, Biothermodynamics: The Study of Biochemical Processes at Equilibrium, John Wiley & Sons, 1983.
[44] J. Wyman and S.J. Gill, in Binding and Linkage: Functional Chemistry of Biological Macromolecules, University Science Books, Mill Valley, CA, 1990.
[45] R.C. Williams and K.Y. Tsay, Anal. Biochem., 54 (1973) 137.
[46] S.H.C. Ip, M.L. Johnson and G.K. Ackers, Biochemistry, 15 (1976) 654.
[47] S.H.C. Ip and G.K. Ackers, J. Biol. Chem., 252 (1977) 82.
[48] G.L. Kellett and H. Gutfreund, Nature, 227 (1970) 921.
[49] B.W. Turner, D.W. Pettigrew and G.K. Ackers, Methods Enzymol., 76 (1981) 596.
[50] G.K. Ackers and M.L. Johnson, Biophys. Chem., 37 (1990) 265.
[51] H. Schonert and B. Stoll, Eur. J. Biochem., 176 (1988) 319.
[52] K. Imai and T. Yonetani, J. Biol. Chem., 250 (1975) 7093.
[53] G.W. Haupt, J. Opt. Soc. Am., 42 (1952) 441.
[54] R.I. Shrager, Chemometrics Intell. Lab. Syst., 1 (1986) 59.
[55] W.H. Press, S.A. Flannery, S.A. Teukolsky and W.T. Vetterling, in Numerical Recipes: The Art of Scientific Computing, Cambridge University Press, Cambridge, 1986.
[56] D.W. Ownby and S.J. Gill, Biophys. Chem., 37 (1990) 395.
[57] E.R. Henry and J. Hofrichter, Methods Enzymol., 210 (1992) 129.
[58] A. Hayashi, T. Suzuki and M. Shin, Biochim. Biophys. Acta, 310 (1973) 310.
[59] M.L. Johnson and S.G. Frasier, Methods Enzymol., 117 (1985) 301.
[60] P.R. Bevington, in Data Reduction and Error Analysis for the Physical Sciences, McGraw-Hill, New York, 1969.
[61] M.L. Doyle and G.K. Ackers, Biophys. Chem., 42 (1992b) 271.
[62] M.L. Doyle, D.W. Myers, G.K. Ackers and R.I. Shrager, Methods Enzymol., 232 (1994) 576.
[63] E. Wilhelm, R. Battino and R. Wilcock, J. Chem. Rev., 77 (1977) 219.
[64] R.C. Weast, CRC Handbook of Chemistry and Physics, 53rd edn., Chemical Rubber Company, 1972, p. D-123.
[65] B. Shaanan, J. Mol. Biol., 171 (1983) 31.
[66] G. Fermi, M.F. Perutz, B. Shaanan and R. Fourme, J. Mol. Biol., 175 (1984) 159.
[67] A. Szabo and M. Karplus, J. Mol. Biol., 72 (1972) 163.
[68] P.W. Roughton and R.L. Lyster, Hvalradets Skr. 48 (1965) 185.
[69] P. Nicholas, M. Cramier, P. Dessen and P. Cohen, J. Biol. Chem., 15 (1976) 3965.
[70] R. Valdes and G.K. Ackers, Proc. Natl. Acad. Sci. U.S.A., 75 (1978) 311.
[71] A. Kurz and C. Bauer, Biochem. Biophys. Res. Commun., 84 (1978) 852.
[72] E. Di Cera, C.H. Robert and S.J. Gill, Biochemistry, 26 (1987) 4003.
[73] Q.E. Gibson and S.J. Edelstein, J. Biol. Chem., 250 (1987) 516.
[74] J. Monod, J. Wyman and J.P. Changeux, J. Mol. Biol., 12 (1965) 88.
[75] G.K. Ackers and M.L. Johnson, J. Mol. Biol., 147 (1981) 554.
[76] J.S. Philo and J.W. Lary, J. Biol. Chem., 265 (1990) 139.
[77] F.R. Smith and K.C. Simmons, Proteins, 18 (1994) 295.
[78] M.L. Johnson, Methods Enzymol., 232 (1994) 597.
[79] A.W. Lee, M. Karplus, C. Poyart and E. Burseaux, Biochemistry, 18 (1988) 1285.
[80] J. Kistar, C. Poyart and S.J. Edelstein, J. Biol. Chem., 262 (1987) 12085.
[81] M.C. Marden, J. Kister and C. Poyart, J. Mol. Biol., 208 (1989) 341.
[82] G.K. Ackers, M.L. Johnson, F.C. Mills, H.R. Halvorson and S. Shapiro, Biochemistry, 14 (1975) 5128.
[83] Y. Huang, M. Koestner and G.K. Ackers, Biophys. J., 71 (1996) 2106.